

Heavy squarks at the LHC

JiJi Fan,^a David Krohn,^b Pablo Mosteiro,^a Arun M. Thalappilil^c and Lian-Tao Wang^{a,c,d}

^a*Department of Physics, Princeton University,
Princeton, NJ, 08540, U.S.A.*

^b*Department of Physics, Harvard University,
Cambridge MA, 02138, U.S.A.*

^c*Enrico Fermi Institute and Department of Physics, University of Chicago,
Chicago, IL, 60637, U.S.A.*

^d*Kavli Institute for Cosmological Physics, University of Chicago,
Chicago, IL, 60637, U.S.A.*

E-mail: jjifan@princeton.edu, dkrohn@physics.harvard.edu,
pablo@princeton.edu, madhav@uchicago.edu, liantaow@uchicago.edu

ABSTRACT: The LHC, with its seven-fold increase in energy over the Tevatron, is capable of probing regions of SUSY parameter space exhibiting qualitatively new collider phenomenology. Here we investigate one such region in which first generation squarks are very heavy compared to the other superpartners. We find that the production of these squarks, which is dominantly associative, only becomes rate-limited at $m_{\tilde{q}} \gtrsim 4(5)$ TeV for $\mathcal{L} \sim 10(100)$ fb⁻¹. However, discovery of this scenario is complicated because heavy squarks decay primarily into a jet and boosted gluino, yielding a dijet-like topology with missing energy (MET) pointing along the direction of the second hardest jet. The result is that many signal events are removed by standard jet/MET anti-alignment cuts designed to guard against jet mismeasurement errors. We suggest replacing these anti-alignment cuts with a measurement of jet substructure that can significantly extend the reach of this channel while still removing much of the background. We study a selection of benchmark points in detail, demonstrating that $m_{\tilde{q}} = 4(5)$ TeV first generation squarks can be discovered at the LHC with $\mathcal{L} \sim 10(100)$ fb⁻¹.

KEYWORDS: Supersymmetry Phenomenology, QCD Phenomenology

ARXIV EPRINT: [1102.0302](https://arxiv.org/abs/1102.0302)

Contents

1	Introduction	1
2	Production rates and branching ratios	3
3	Analysis	5
3.1	Pre-selection cuts and backgrounds	5
3.2	E_T -jet alignment cuts	7
3.3	Jet substructure variables	7
3.4	Final cuts	10
3.5	Uncertainties	10
4	Conclusion	12

1 Introduction

The Large Hadron Collider (LHC) has commenced operation and is already producing collisions at energies far above the scale of electroweak symmetry breaking (EWSB). Thus one can be hopeful that soon the particle responsible for EWSB (e.g. the Higgs) will be discovered, as well as any physics beyond the standard model (BSM) responsible for setting the scale at which this breaking occurs.

Supersymmetry (SUSY) is perhaps the most promising candidate for BSM physics, and as such its phenomenology has been studied extensively. However, the SUSY parameter space is so complicated that most collider studies confine themselves to studying a restrictive subset of models or simple benchmark points (e.g. mSUGRA [1] and the SPS points [2], respectively). In general though, it is useful to look at other regions of parameter space to make sure no signals are missed [3, 4].

Here we will focus on one such understudied region in which first generation squarks are very heavy compared to the other SUSY superpartners.¹ This scenario deserves attention not only because it yields a viable SUSY spectrum, but also because it is motivated by many interesting SUSY scenarios [5, 6] including more recent work in split SUSY [7–9], PeV-scale SUSY [10], and single sector SUSY breaking [11, 12]. Intuitively, it is reasonable to anticipate heavy first generation squarks because they play a minimal role in solving the hierarchy problem (i.e. stabilizing the electroweak scale) - only the third generation really needs to be light if SUSY plays the role we expect of it. In any case, here our main goal

¹We focus on first generation squarks because they result mostly from the scattering of valence quarks, and are thus produced in much greater numbers than squarks of the second and third generation. Furthermore, we note that while our squarks are heavy the gluinos are not unusually long-lived, i.e. we are not considering a situation with R-hadrons.

is to determine an optimal search strategy for discovering heavy squarks and to assess the reach of the LHC in finding them.

Now, when squarks are very heavy it becomes too costly to create them in pairs and so heavy squarks are dominantly produced in association with a different superpartner. This associated particle is usually the gluino, due to its large color charge. Furthermore, once produced the squark usually decays into a gluino and a jet, again because of the gluino's large color charge, yielding the topology:

$$pp \rightarrow \tilde{q}\tilde{g} \tag{1.1}$$

$$\hookrightarrow 2\tilde{g} + j.$$

Since, in most plausible SUSY spectra, all superpartner decays yield a stable neutral particle (i.e. the LSP, labeled $\tilde{\chi}_1^0$) squark associated production would seem to yield the classic new physics signal: jets + \cancel{E}_T . However, for heavy squark scenarios, new challenges appear in this well-studied final state.

Difficulties arise because the gluino from the decaying squark will be very energetic (assuming $m_{\tilde{g}} \ll m_{\tilde{q}}$), and so all of its decay products become collimated, confined to a cone of opening angle

$$\Delta R \sim \frac{2m_{\tilde{g}}}{p_T} \sim \frac{m_{\tilde{g}}}{m_{\tilde{q}}}. \tag{1.2}$$

In practice, this means that the boosted gluino's decay products will often be resolved as a single jet (henceforth the *gluino jet*). Furthermore, although there are two sources of \cancel{E}_T in this process, the $\tilde{\chi}_1^0$ from the boosted gluino is much harder than that of the associated gluino, and so the \cancel{E}_T in this process tends to be aligned with the gluino jet. Thus, what is really a complicated SUSY process is resolved as two back-to-back jets with \cancel{E}_T aligned along one of them - the telltale signature of a mismeasured QCD dijet event. Indeed, precisely because our signal events look so much like QCD dijets they are often vetoed by standard pre-selection cuts. Traditionally one requires a separation in azimuthal angles between the \cancel{E}_T and any nearby jets in order to remove mismeasurement backgrounds: D0 requires $\Delta_\phi(\cancel{E}_T, j) > 0.8$ in its jets + \cancel{E}_T search [13], while the LHC experiments require $\Delta_\phi(\cancel{E}_T, j) \gtrsim 0.3$ [14]. We therefore expect to run into trouble using standard analyses when $m_{\tilde{g}}/m_{\tilde{q}} \lesssim 0.3$.

It is clear that to resolve heavy squarks at the LHC the cut on $\Delta_\phi(\cancel{E}_T, j)$ should be relaxed and some other tool must be used to remove mismeasured QCD. Here we propose using jet substructure² for this purpose. This approach is motivated by the fact that while the four-momentum of a gluino jet could be similar to that of a QCD jet, the distribution of the constituent four-momenta *inside* the jet (i.e. the calorimeter cells inside of it) will be very different. Gluino jets contain many hard, widely separated subclusters of energy, evidence of a decay chain, while the depositions within a QCD jet assume a hierarchical structure, evidence for emissions governed by the showering of partons within QCD. The variables of jet substructure allow one to distinguish between these two cases, as we will soon see.

²For a review of these techniques, see refs. [15, 16].

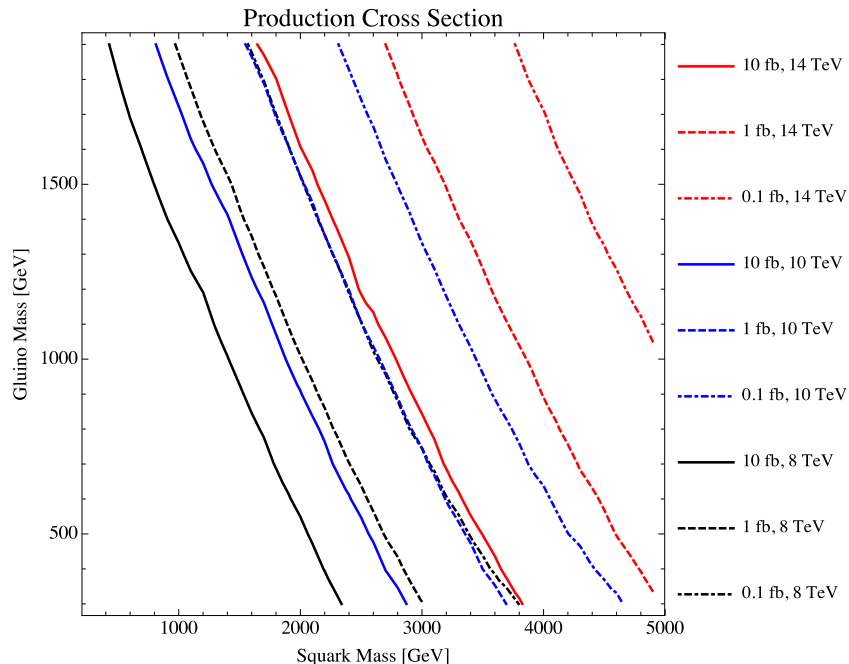


Figure 1. The leading order cross-section for $\tilde{q} + \tilde{g}$ associated production at different $(m_{\tilde{q}}, m_{\tilde{g}})$ for a $\hat{s} = 14, 10, 8$ TeV LHC (red, blue, black) where $\sigma = 10, 1, 0.1$ fb boundaries are indicated by solid, dashed, and dot-dashed lines, respectively.

The paper is structured as follows. In section 2 we discuss squark production rates and decay channels. Section 3 studies the basic kinematic cuts necessary to discover heavy squarks over the SM backgrounds and discusses jet substructure observables helpful in reducing mismeasurement errors. Finally, we conclude in section 4.

2 Production rates and branching ratios

In determining the reach of the LHC in probing heavy squarks the place to start, of course, is with production rates. As mentioned in the introduction, heavy squarks are dominantly produced in association with one of the lighter superpartners simply because pair production would require a very high energy, the probability of which is suppressed by the fast-falling nature of the proton’s parton distribution functions (PDFs). Furthermore the state produced in association with the squark is almost always a gluino because of its large coupling.

In figure 1 we plot the leading order³ cross section for the process $pp \rightarrow \tilde{q} + \tilde{g}$ over a range of $(m_{\tilde{q}}, m_{\tilde{g}})$ and at different LHC energies. These results are obtained using `Pythia v6.423` [18] assuming the first generation squarks are all degenerate in mass and any mixings are negligible. If we require $S/\sqrt{B} > 5$ with at least 10 signal events [19] for discovery, then one can see that for $\mathcal{L} \sim 10(100)$ fb⁻¹ a 14 TeV LHC is in principle capable of discovering squarks up to $m_{\tilde{q}} \sim 4(5)$ TeV.

³The NLO calculation is given in [17].

Once heavy squarks are produced they will dominantly decay through the QCD channel $\tilde{q} \rightarrow q\tilde{g}$ which will be the focus of our study, although some squarks will decay into neutralinos or charginos.⁴ Of course, once gluinos have been produced they too decay. Fortunately, gluino decays in models with heavy squarks have been well studied in the literature [20, 21]. In general, there are three major decay chains for the gluino:

1. Via an off-shell squark to two quarks and the LSP: $\tilde{g} \rightarrow q\bar{q} + \tilde{\chi}_1^0$.
2. Via an off-shell squark to two quarks and a chargino or heavier neutralino: e.g. $\tilde{g} \rightarrow q\bar{q} + \tilde{\chi}_1^\pm$.
3. Through a squark-quark loop: $\tilde{g} \rightarrow g + \tilde{\chi}_1^0$.

The explicit formulae of the decay widths can be found in ref. [20]. A few remarks are in order:

- We note that the $q\bar{q}$ pair formed from the decay of the gluino can, if kinematically allowed, be composed of top quarks. This results in an even richer jet substructure than the decay to light quarks. In fact, as one expects the stop squark to be relatively light (as it plays a large role in stabilizing the Higgs mass), and the decay widths scale as $1/m_{\tilde{q}}^4$, the branching ratio to the ditop channel $\tilde{g} \rightarrow t\bar{t} + \tilde{\chi}_1^0$ can often dominate.
- In the limit where $\tilde{\chi}_1^0$ is purely a Bino, the squark mass matrices are flavor-diagonal, and left-right mixings are negligible, the ratio of the 2-body decay rate to that of the 3-body decays, $R_{2/3} \equiv \Gamma(\tilde{g} \rightarrow 2 \text{ body}) / \Gamma(\tilde{g} \rightarrow 3 \text{ body})$ is

$$R_{2/3} \propto \sum_{\text{flavors}} \frac{\alpha_s (m_L^2 - m_R^2)^2}{m_L^4 + m_R^4} \quad (2.1)$$

In this limit, the loop-induced decay $\tilde{g} \rightarrow g + \tilde{\chi}_1^0$ is suppressed by the mass splitting between the left- and right- handed squarks $m_L^2 - m_R^2$. This is because $\tilde{g} \rightarrow g + \tilde{B}$, governed by the magnetic operator $\tilde{\chi}_1^0 \sigma^{\mu\nu} \gamma_5 \tilde{g} G_{\mu\nu}$, is a C-violating process. It vanishes for pure strong interactions with degenerate squark masses as these preserve C-parity. Any such C-violating decay channel can only be generated by the weak interactions which generate the mass splittings between squarks of different handedness.

- Finally, another interesting limit emphasized in [20] is when the gluino is kinematically allowed to decay into Higgsinos. Here the radiative decay is enhanced by $(\log(m_{\tilde{t}}/m_t))^2$ due to the stop and top loop.

For our study, we will take the mass differences between $m_L^2 - m_R^2$ to be negligible compared to the squark mass, and we will posit that gluino decays to Higgsinos are kinematically forbidden. Thus, in what follows we will be considering only gluino three-body decays.

⁴In our simulations we will account for the suppressed branching $\tilde{q} \rightarrow \tilde{g} + q$ due to decays into electroweak superpartners. However, the effects of this suppression are small.

Model	$m_{\tilde{g}}$ [GeV]	$m_{\tilde{\chi}_1^0}$ [GeV]	\tilde{g} decay channel	$\text{Br}(\tilde{q} \rightarrow \tilde{g} + q)[\%]$
1	400	150	$\tilde{g} \rightarrow jj\tilde{\chi}_1^0$	88 (88)
2	400	100	$\tilde{g} \rightarrow jj\tilde{\chi}_{2,3,4}^0 \rightarrow jj\tilde{\chi}_1^0 Z/h$ $\tilde{g} \rightarrow jj\tilde{\chi}_{1,2}^\pm \rightarrow jj\tilde{\chi}_1^0 W^\pm$	78 (77)
3	600	150	$\tilde{g} \rightarrow t\bar{t}\tilde{\chi}_1^0$	76 (82)

Table 1. The three benchmark SUSY models we will consider. In the last column, where we have listed the branching ratio for the decay of the squark into a gluino, the number outside of parenthesis is for $m_{\tilde{q}} = 4$ TeV and the number inside is for $m_{\tilde{q}} = 5$ TeV.

3 Analysis

To study the phenomenology of the different gluino decay possibilities discussed in section 2 we choose the three benchmark models presented in table 1. We will study each of these points at $m_{\tilde{q}} = 4$ TeV and 5 TeV. These points include the decay of the gluino into two light jets + $\tilde{\chi}_1^0$, the cascade decay into heavy electroweak particles along with two jets and a $\tilde{\chi}_1^0$, and the decay into top pairs with a $\tilde{\chi}_1^0$. These decay chains are realized by spectra with $2m_t, m_{\text{ino}} > m_{\tilde{g}} - m_{\tilde{\chi}_1^0}$ (model 1), $m_{\text{ino}} < m_{\tilde{g}} - m_{\tilde{\chi}_1^0}$ (model 2), and a light stop with $2m_t < m_{\tilde{g}} - m_{\tilde{\chi}_1^0}$ (model 3) where m_{ino} is the mass of the second-lightest non-colored ino. While all of these models illustrate only one decay chain, it is certainly possible for nature to manifest some admixture of the three. However, as we will see, as all decay chains are discoverable with a comparable integrated luminosity (the main difference in final significance will come from a difference in rates due to the difference in gluino masses) this should not have any significant effect upon our conclusions. Finally, we note that all of these points are consistent with existing studies which place bounds on $m_{\tilde{g}}$ and $m_{\tilde{\chi}_1^0}$ using Tevatron data on jets + \cancel{E}_T [22].

3.1 Pre-selection cuts and backgrounds

To begin we define a set of pre-selection cuts which roughly characterize the kinematic features of the signal. This will allow us to focus on the most relevant backgrounds. Since we study benchmark models with heavy squarks at $m_{\tilde{q}} = 4$ TeV and 5 TeV, which then decay into an ordinary QCD jet and a gluino jet, our signal is characterized by jets and missing energy. We therefore require:

- $p_T(j_1) > 1.5$ TeV
- $p_T(j_2) > 400$ GeV
- $\cancel{E}_T > 500$ GeV.

where we use j_i to denote the i -th hardest jet. With these pre-selection cuts there are three major sources of background:

1. The most obvious background given the pre-selection cuts above is $Z/W + \text{jets}$ where $Z \rightarrow \nu\bar{\nu}$ or $W \rightarrow l\nu$.⁵ It is worthwhile to emphasize that the effects of this background are somewhat non-standard for heavy-squark signals. Normally the $Z/W + \text{jets}$ background can be significantly reduced via a cut on how dijet-like an event is (e.g. the α variable of ref. [25]) as SUSY events, which usually have two or more sources of \cancel{E}_T , look less dijet-like than SM events.⁶ Here however, because the BSM events we study appear dijet-like, such a cut cannot be imposed without removing a significant portion of the signal.
2. Another important background comes from boosted $t\bar{t}$ production. Here \cancel{E}_T can arise when one top decays semi-leptonically and the resulting lepton becomes difficult to distinguish from the b -jet (due to their collimation). Just as with the leptonic decays of the W in $W + \text{jets}$ production, here the lepton can become collimated with a jet. As discussed in ref. [27], the lepton and the b quark from a boosted top decay will be within $\Delta R = 0.4$ of each other roughly 50% of the time when $p_T \sim 1$ TeV, and nearly 100% of the time when $p_T \sim 2$ TeV. Due to this collimation, the resulting leptons will not pass isolation cuts and the events could be resolved as simply jets + \cancel{E}_T . As with the $W + \text{jets}$ background, here we will take a conservative approach and cluster non-isolated leptons into jets.
3. Finally, QCD multijet events can contribute to our background in two ways. Dijet events can contribute real missing energy when they fragment into b -hadrons, which can decay semi-leptonically. Furthermore, dijet events can yield fake missing energy when they are mismeasured. Here we will simulate the effects of the first type of contribution (semi-leptonic b -hadron decays) and provide efficiency estimates for methods to reduce the second type of decay.⁷

Before proceeding, we note that in what follows our signal events are generated at parton level using `Madgraph v4.4.49` [28], showered in `Pythia v6.422` [18], and matched using the MLM procedure [29]. Some of our backgrounds (multi-jets and $Z + \text{jets}$) are simulated in `Sherpa 1.2.3` [30] using the package's automated CKKW matching [31], while others ($t\bar{t}$ and $W + \text{jets}$) are simulated using the same Madgraph/Pythia flow with MLM matching that we used to generate our signal. When we have run checks comparing Madgraph with MLM matching to Sherpa with CKKW, we find they agree with each other

⁵While $W \rightarrow l\nu$ backgrounds can normally be removed from jets + \cancel{E}_T samples via a cut on isolated leptons, here we will find the lepton from the W decay is often collimated with a jet and thus non-isolated. While identifying collimated leptons may be possible (see, for example, refs. [23, 24]), to be conservative we will simply consider leptons as part of jets when they are close enough to be clustered with them.

⁶It is also worth mentioning that the cross section for $Z + \text{jets}$ can be surprisingly large when the Z is allowed to be collinear with a jet [26]. For configurations like these the events are, morally speaking, dijet QCD events where a jet radiates a Z , leading to a $\ln^2 p_T/m_Z$ enhancement.

⁷In the kinematic region we are considering, where \cancel{E}_T is large compared to jet p_T s, any mismeasurement error is non-gaussian and would require a more detailed detector simulation than we can confidently provide. Therefore, we do not attempt to simulate this sort of mismeasured event - instead, later we only provide efficiency estimates.

	Model 1	Model 2	Model 3	$Z + J$	$W + J$	$t\bar{t}$	QCD
No cuts	4.26 (0.51)	3.78 (0.45)	1.78 (0.23)	-	-	-	-
Pre-selection (PS)	1.72 (0.27)	1.46 (0.23)	0.78 (0.14)	0.43	1.05	0.41	0.82
PS & $\Delta\phi(\cancel{E}_T, j) > 0.3$	0.67 (0.09)	0.47 (0.06)	0.31 (0.05)	0.24	0.54	0.01	0.03
PS & $y_{1\rightarrow 2} > 2 \cdot 10^{-3}$	1.13 (0.18)	1.15 (0.18)	0.73 (0.12)	0.07	0.32	0.18	0.17
PS & $y_{1\rightarrow 2} > 2 \cdot 10^{-3}$ & $p_T(j_3) > 100$ GeV	0.97 (0.16)	1.01 (0.16)	0.68 (0.11)	0.04	0.18	0.06	0.09

Table 2. Signal (for $m_{\tilde{q}} = 4(5)$ TeV) and background cross sections, in fb, in the presence of various cuts.

within roughly 20% for most distributions. After generation, all events are clustered into jets by `Fastjet v2.4.2` [32, 33] using the anti- k_T algorithm [34] with $R = 0.7$.

3.2 \cancel{E}_T -jet alignment cuts

The initial signal cross sections (after accounting for the gluino branching ratio), as well as the signal and background rates resulting from the pre-selection cuts introduced earlier, are shown in table 2. Using the pre-selection cuts we see that the signal rates are reduced by roughly 60%, but the background are brought to the fb level. Furthermore, as can be seen in figure 2, the signal and background are both primarily dijet like (since $\Delta\phi(j_1, j_2) \sim \pi$) and \cancel{E}_T is mostly aligned with the second hardest jet.

As discussed earlier, in addition to the cuts already imposed it is customary to apply a cut on jet- \cancel{E}_T alignment requiring $\Delta\phi(j, \cancel{E}_T) \gtrsim 0.3$. However, as can be seen on the right hand side of figure 2, and in table 2, such a cut would reduce signal rates by 60 – 70%. While the $\Delta\phi(j, \cancel{E}_T)$ cut does reduce background (especially the QCD background, which goes down by $\sim 96\%$), such a cut is impractical and we must relax it, replacing it with something else.

3.3 Jet substructure variables

As emphasized in the introduction, the gluino jets in our signal events have a rich substructure. Here we will investigate observables sensitive to this substructure and use them to replace cuts on $\Delta\phi(\cancel{E}_T, j)$.

The basic idea behind jet substructure methods is that the distribution of constituent cells/particles inside the jets of boosted heavy objects (like the gluino) is different than in ordinary QCD jets. Basically, boosted objects tend to undergo a decay at a fixed order to partons of roughly equal energy (e.g. the top decay $t \rightarrow 3j$), while the jets from light particles radiate in a probabilistic fashion and with a strong energy hierachy. This observation has been used to identify and study boosted EW gauge bosons [35–39], higgses [40–45], tops [46–54], and other exotica [55–59]. For a review, see refs. [15, 16].

A particularly simple observable sensitive to jet substructure is the z variable of ref. [47]. To calculate z for a jet, one takes its constituents, reclusters them using the k_T -algorithm [60, 61], and unwinds the clustering one step so that there are two subjets,

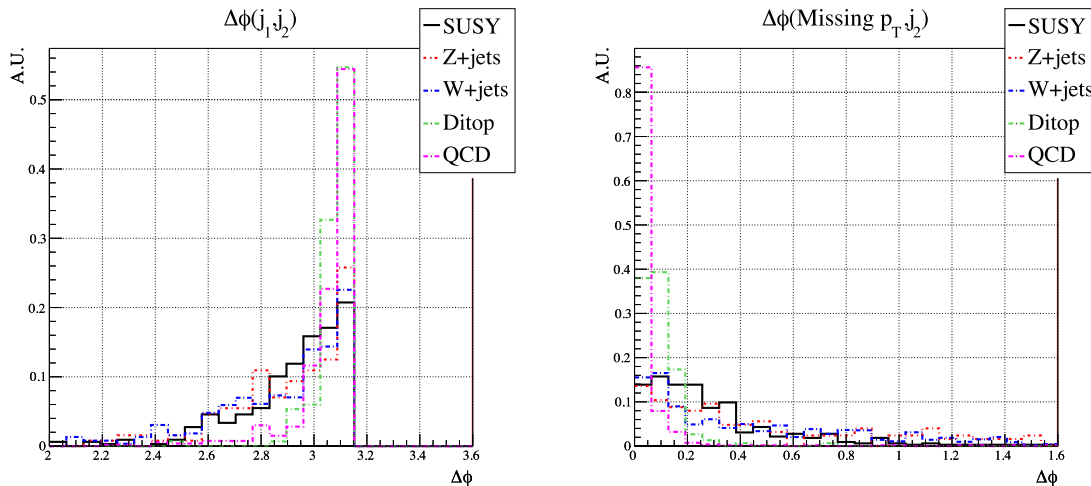


Figure 2. $\Delta\phi(j_1, j_2)$ and $\Delta\phi(\cancel{E}_T, j_2)$ distributions on the left and right after the pre-selection cuts have been applied. The distribution labeled “SUSY” is for a $m_{\tilde{q}} = 4$ TeV squark decaying to light flavor: $\tilde{q} \rightarrow q\bar{q}\chi_0^1$ (Model 1). However, we note that the distributions using other gluino decay modes are quite similar. Note that all histograms are normalized to the same area.

A and B . Then, z is defined as

$$z = \frac{\min(E_A, E_B)}{E_A + E_B} \tag{3.1}$$

where E_A and E_B are the energies of the two subjects. When the k_T -algorithm acts on the constituent four-momenta (e.g. calorimeter cells) of a jet, it does so by computing a distance between each pair of four-momenta using the metric

$$d_{ij} = \min(p_{Ti}^{-2}, p_{Tj}^{-2}) \left(\frac{\Delta R}{R_0} \right)^2, \tag{3.2}$$

for ΔR the angular distance between two jets and R_0 a constant. The smallest of these distance measures is chosen, and the four-momenta associated with it are combined together. In this way a jet is built up in stages, from soft to hard and in angle from near to far. Now, the angle and energy sharing of the radiation emitted by quarks and gluons has a soft/collinear singularity⁸ and thus z , which measures this energy sharing is ~ 0 for ordinary QCD jets, while boosted heavy objects, which have no such singularity,⁹ yield $z \sim 1/2$.

The distributions of z for our signal and background processes are shown in figure 3. Here we see that, as expected, the hard splitting present in the signal processes can be distinguished from the soft/collinear splitting of QCD.

However, it is possible to do better. The z variable measures only the energy sharing of the subjects when a jet is broken in two - it only provides minimal information about the

⁸I.e. a gluon tends to split into two gluons, where one is very soft and/or collinear with the other.

⁹E.g. because $h \rightarrow b\bar{b}$ decays isotropically in its rest frame it has no singularity when one of the b s becomes soft.

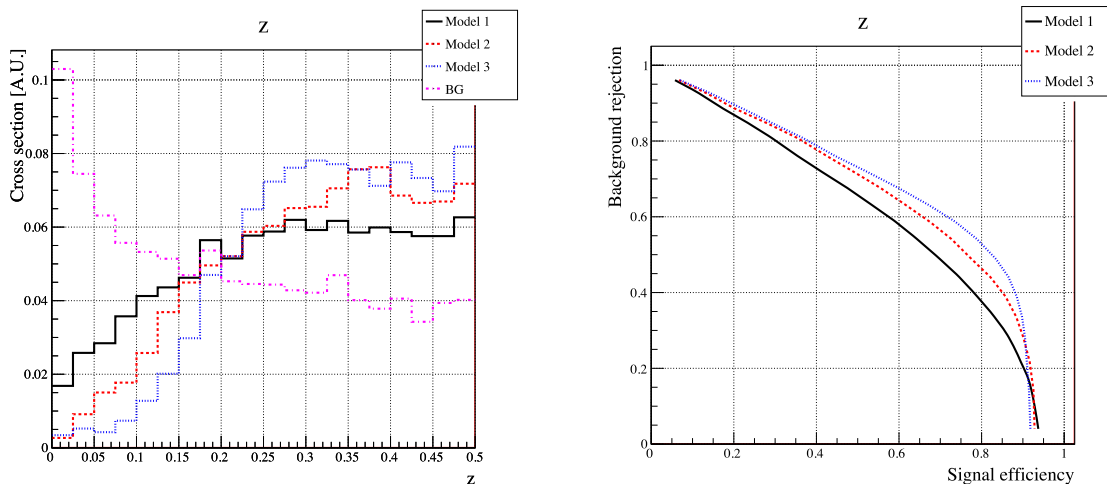


Figure 3. On the left, the distribution of the z variable of ref. [47], and on the right, the signal and background efficiencies obtained with it. An 80% signal efficiency requires a cut on z of 0.14/0.16/0.21 for models 1/2/3, respectively.

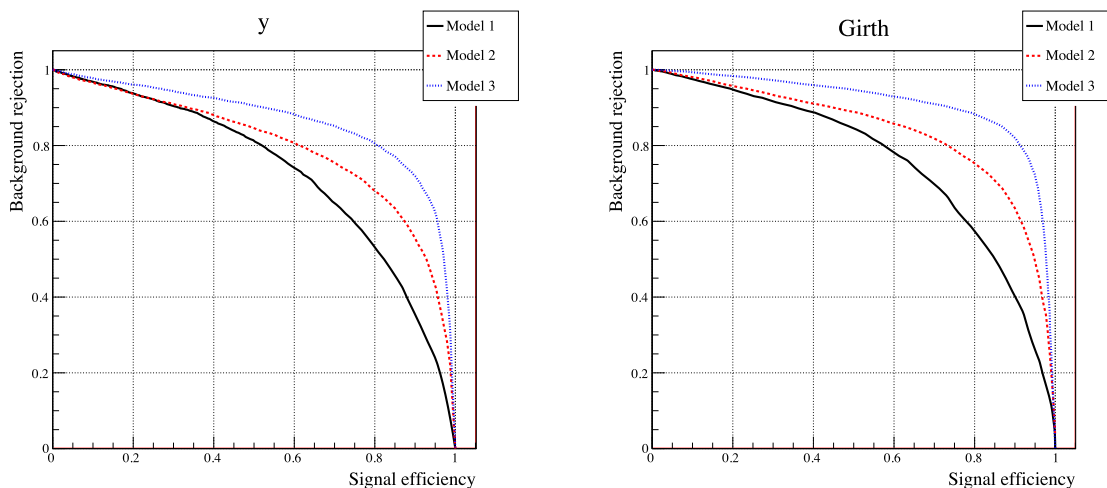


Figure 4. Signal and background efficiencies computed using, on the left, the of eq. (3.3), and on the right the girth variable of eq. (3.4). An 80% signal efficiency requires a cut on y of $(1.2/2.3/4.3) \cdot 10^{-3}$ or a cut on girth of $(0.9/1.4/1.9) \cdot 10^{-1}$ for models 1/2/3, respectively.

angular dependence.¹⁰ However, the y variable introduced in ref. [37]

$$y_{1 \rightarrow 2} = \frac{d_{1 \rightarrow 2}}{p_T^2} \tag{3.3}$$

for $d_{1 \rightarrow 2}$ the scale at which the initial jet is broken into two (see eq. 3.2) contains this information. The resulting efficiency curves obtained from cuts using this variable are presented in figure 4. One can see a marked improvement over the results obtained with the z variable. Using $y_{1 \rightarrow 2}$ it is possible to obtain over 90% background rejection with greater than $\sim 40\%$ signal acceptance (and even 60% signal acceptance for $\tilde{g} \rightarrow t\bar{t}$).

¹⁰The k_T algorithm makes use of angular information when constructing the two subjects.

Finally, we note that it is possible to detect jet substructure without directly constructing subjects. Ref. [62] introduced a jet shape variable termed girth:

$$g = \frac{1}{p_T} \sum r_i p_{T,i}, \tag{3.4}$$

where the sum is taken over all jet constituents and r_i is the distance from each to the jet center. By making the replacements $E \rightarrow p_T$ and $\theta \rightarrow r$, one can see girth is analogous to the ‘jet broadening’ [63] shape used at e^+e^- colliders. The efficiencies obtained through the application of girth are shown in figure 4. They are even better than the efficiencies obtained with the y variable (although in what follows we will make use of the y variable, as it is more widely used). Before closing, we note that while these are not completely independent variables, they have different strengths and sensitivities to contamination, and thus a more detailed experimental study is needed to optimize a cut on substructure. In closing, we note that the recently introduced N -subjettiness [64, 65] variables might also be useful for this purpose.

3.4 Final cuts

We now apply a substructure cut ($y_{1 \rightarrow 2} > 2 \cdot 10^{-3}$) in addition to the pre-selection cuts used earlier to find the efficiencies listed in table 2. From these efficiencies we see that the substructure cut removes a significant amount of the background (the QCD rate drops 79%) while much of the signal is retained (only dropping 20 – 30%). However, the background levels are still worrisome, in particular for $W + \text{jets}$.

Fortunately, we can still cut on the subleading jets. Even though our signal is dominantly dijet like, the gluino produced in association with the squark decays largely into jets which are harder than those characteristic of the background. This can be seen in figure 5, where we show the p_T of the third hardest jet in the events. After imposing a cut on the third hardest jet (we use $p_T(j_3) > 100$ GeV) we find the background has been reduced to the point where all three $m_{\tilde{q}} = 4$ TeV models can be seen at 5σ in 10 fb^{-1} of data (see table 2 and table 3). It is interesting to note that after all of these cuts the three backgrounds contribute comparably.

Finally, we observe that while the cuts so far are insufficient to see $m_{\tilde{q}} = 5$ TeV squarks in 100 fb^{-1} of data, this can be remedied by increasing the jet p_T cuts slightly to account for the higher squark mass. Indeed, we find that simply increasing the cut on $p_T(j_1)$ from 1.5 to 2 TeV we reduce the background enough (by 86%) to see the heavier squarks.¹¹ The final cross sections and LHC sensitivity can be seen in table 3.

3.5 Uncertainties

In closing, we comment on theoretical and experimental uncertainties in our analysis which have the potential to affect the reach presented in table 3.

We expect the principle source of theoretical uncertainties in our analysis to apply to the production rates we use since these are all calculated at tree level. According to ref. [66],

¹¹We emphasize though that this higher cut on the leading jet p_T is detrimental to the search for $m_{\tilde{q}} = 4$ TeV squarks, and for these a cut of 1.5 TeV should be used.

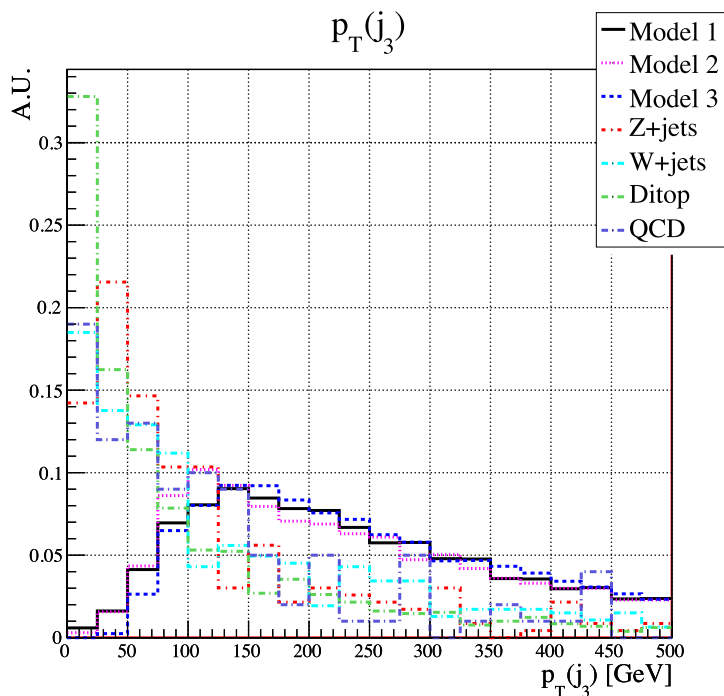


Figure 5. p_T of the third hardest jet for different signal models (all with $m_{\tilde{q}} = 4$ TeV) after applying the pre-selection cuts defined earlier, along with a cut requiring $y_{1 \rightarrow 2} > 2 \cdot 10^{-3}$ for the second hardest jet.

	Model 1	Model 2	Model 3
σ_S	0.97 (0.11)	1.01 (0.11)	0.68 (0.08)
S/\sqrt{B}	5.0 (4.9)	5.3 (4.9)	3.5 (3.6)

Table 3. Signal cross section and significance for $m_{\tilde{q}} = 4(5)$ TeV at $\mathcal{L} = 10(100)$ fb $^{-1}$. To arrive at these numbers we use the preselection cuts defined earlier (increasing the cut on $p_T(j_1)$ to 2 TeV for $m_{\tilde{q}} = 5$ TeV) and required $p_T(j_3) > 100$ GeV and $y_{1 \rightarrow 2}(j_2) > 2 \cdot 10^{-3}$. Note that, after applying these cuts we found background cross sections of $\sigma_B = 0.37(0.05)$ fb.

the NLO K -factors relevant to $V + \text{jets}$ and $t\bar{t}$ production are $\mathcal{O}(0.9 - 1.5)$ while ref. [17] shows K -factors for squark-gluino production rising with $m_{\tilde{q}}$ which at $m_{\tilde{q}} = 1$ TeV¹² are generally $\mathcal{O}(1.5)$. We therefore expect that our quoted values for S/\sqrt{B} will likely increase slightly once we calculate at higher orders, but even taking a very conservative standpoint it is hard to see these decreasing beyond more than 20% of the values we quote. In any case, the squark production rates fall so fast with mass that even a relatively large $\mathcal{O}(50\%)$ shift in S/\sqrt{B} would only shift the mass reach by a much smaller factor, probably only $\mathcal{O}(10\%)$.

As for the experimental uncertainties affecting our analysis, we believe these will be minimal when compared to the theoretical uncertainties. The jets we consider are so hard there should be no issues with trigger efficiencies, and as the signal distribution of \cancel{E}_T is not steeply falling where we cut it (500 GeV) the uncertainties in jet resolution which can affect

¹²Explicit numbers are not provided for squarks as heavy as those we consider.

this measurement should be below the tens of percent uncertainties coming from NLO corrections. Finally, recent calibrations (ref. [67]) have shown good agreement between substructure methods and LHC data - we therefore expect only minimal uncertainties to result from the application of the substructure techniques we present.

4 Conclusion

Here we have considered a relatively unstudied region of SUSY parameter space exhibiting interesting collider phenomenology. In the region we investigated first generation squarks are very heavy, leading to signal events which appear dijet like with \cancel{E}_T aligned with a jet. We found that while we were able to go far in reducing the background to this channel via cuts on jet $p_{T\text{s}}$ and \cancel{E}_T , much of our signal was removed by jet/ \cancel{E}_T anti-alignment cuts used by LHC experiments to guard against jet mismeasurement errors.

We suggested replacing these cuts by a measurement of jet substructure. This allowed us to still remove much of the background while retaining a substantial portion of the signal. After applying this and the aforementioned cuts, we demonstrated heavy squarks could be seen at $m_{\tilde{q}} = 4(5)$ TeV in $\mathcal{L} \sim 10(100)$ fb $^{-1}$ of data. Interestingly, in the end all of our background contributed equally, motivating the need for a careful experimental study of the relevant efficiencies (so as to avoid an unfortunate Altarelli cocktail).

In closing, we note that it would be interesting to see if other signals could be enhanced by replacing anti-alignment and similar cuts on jet quality cuts by measurements of jet substructure. In addition, the backgrounds we encountered could potentially be reduced even more through cuts on non-isolated leptons. We hope this serves as further motivation for experimental study of this interesting configuration.

Acknowledgments

The authors would like to thank N. Arkani-Hamed for suggesting this topic, and G. Salam, M. Schwartz, B. Tweedie, and Z. Han for useful discussions. J.F. is supported by the NSF under grant PHY-0756966. D.K. is supported by a Simons postdoctoral fellowship and by an LHC-TI travel grant. A.T. is supported in part by the DOE under Grant No. DE-FG02-90ER40560. L.-T.W. is supported by the NSF under grant PHY-0756966 and the DOE Early Career Award under grant DE-SC0003930.

References

- [1] A.H. Chamseddine, R.L. Arnowitt and P. Nath, *Locally supersymmetric grand unification*, *Phys. Rev. Lett.* **49** (1982) 970 [[SPIRES](#)].
- [2] B.C. Allanach et al., *The Snowmass points and slopes: Benchmarks for SUSY searches*, *Eur. Phys. J. C* **25** (2002) 113 [[hep-ph/0202233](#)] [[SPIRES](#)].
- [3] C.F. Berger, J.S. Gainer, J.L. Hewett and T.G. Rizzo, *Supersymmetry without prejudice*, *JHEP* **02** (2009) 023 [[arXiv:0812.0980](#)] [[SPIRES](#)].
- [4] J.A. Conley, J.S. Gainer, J.L. Hewett, M.P. Le and T.G. Rizzo, *Supersymmetry without prejudice at the LHC*, [arXiv:1009.2539](#) [[SPIRES](#)].

- [5] R. Barbieri, G.R. Dvali and L.J. Hall, *Predictions from a U(2) flavour symmetry in supersymmetric theories*, *Phys. Lett. B* **377** (1996) 76 [[hep-ph/9512388](#)] [[SPIRES](#)].
- [6] A.G. Cohen, D.B. Kaplan and A.E. Nelson, *The more minimal supersymmetric standard model*, *Phys. Lett. B* **388** (1996) 588 [[hep-ph/9607394](#)] [[SPIRES](#)].
- [7] N. Arkani-Hamed and S. Dimopoulos, *Supersymmetric unification without low energy supersymmetry and signatures for fine-tuning at the LHC*, *JHEP* **06** (2005) 073 [[hep-th/0405159](#)] [[SPIRES](#)].
- [8] G.F. Giudice and A. Romanino, *Split supersymmetry*, *Nucl. Phys. B* **699** (2004) 65 [[hep-ph/0406088](#)] [[SPIRES](#)].
- [9] N. Arkani-Hamed, S. Dimopoulos, G.F. Giudice and A. Romanino, *Aspects of split supersymmetry*, *Nucl. Phys. B* **709** (2005) 3 [[hep-ph/0409232](#)] [[SPIRES](#)].
- [10] J.D. Wells, *PeV-scale supersymmetry*, *Phys. Rev. D* **71** (2005) 015013 [[hep-ph/0411041](#)] [[SPIRES](#)].
- [11] S. Franco and S. Kachru, *Single-sector supersymmetry breaking in supersymmetric QCD*, *Phys. Rev. D* **81** (2010) 095020 [[arXiv:0907.2689](#)] [[SPIRES](#)].
- [12] N. Craig, R. Essig, S. Franco, S. Kachru and G. Torroba, *Dynamical supersymmetry breaking, with flavor*, *Phys. Rev. D* **81** (2010) 075015 [[arXiv:0911.2467](#)] [[SPIRES](#)].
- [13] D0 collaboration, V.M. Abazov et al., *Search for squarks and gluinos in events with jets and missing transverse energy using 2.1 fb⁻¹ of p \bar{p} collision data at $\sqrt{s} = 1.96$ TeV*, *Phys. Lett. B* **660** (2008) 449 [[arXiv:0712.3805](#)] [[SPIRES](#)].
- [14] CMS collaboration, G.L. Bayatian et al., *CMS technical design report, volume II: physics performance*, *J. Phys. G* **34** (2007) 995 [[SPIRES](#)].
- [15] A. Abdesselam et al., *Boosted objects: a probe of beyond the standard model physics*, [arXiv:1012.5412](#) [[SPIRES](#)].
- [16] G.P. Salam, *Towards jetography*, *Eur. Phys. J. C* **67** (2010) 637 [[arXiv:0906.1833](#)] [[SPIRES](#)].
- [17] W. Beenakker, R. Hopker, M. Spira and P.M. Zerwas, *Squark and gluino production at hadron colliders*, *Nucl. Phys. B* **492** (1997) 51 [[hep-ph/9610490](#)] [[SPIRES](#)].
- [18] T. Sjöstrand, S. Mrenna and P.Z. Skands, *PYTHIA 6.4 physics and manual*, *JHEP* **05** (2006) 026 [[hep-ph/0603175](#)] [[SPIRES](#)].
- [19] ATLAS collaboration, *ATLAS detector and physics performance: technical design report 2*, [CERN-LHCC-99-015](#) (1999).
- [20] M. Toharia and J.D. Wells, *Gluino decays with heavier scalar superpartners*, *JHEP* **02** (2006) 015 [[hep-ph/0503175](#)] [[SPIRES](#)].
- [21] P. Gambino, G.F. Giudice and P. Slavich, *Gluino decays in split supersymmetry*, *Nucl. Phys. B* **726** (2005) 35 [[hep-ph/0506214](#)] [[SPIRES](#)].
- [22] J. Alwall, M.-P. Le, M. Lisanti and J.G. Wacker, *Model-independent jets plus missing energy searches*, *Phys. Rev. D* **79** (2009) 015005 [[arXiv:0809.3264](#)] [[SPIRES](#)].
- [23] ATLAS collaboration, *Reconstruction of high mass $t\bar{t}$ resonances in the lepton+jets channel*, [ATL-COM-PHYS-2009-255](#) (2009).

- [24] B. Lillie, L. Randall and L.-T. Wang, *The bulk RS KK-gluon at the LHC*, *JHEP* **09** (2007) 074 [[hep-ph/0701166](#)] [[SPIRES](#)].
- [25] L. Randall and D. Tucker-Smith, *Dijet searches for supersymmetry at the LHC*, *Phys. Rev. Lett.* **101** (2008) 221803 [[arXiv:0806.1049](#)] [[SPIRES](#)].
- [26] M. Rubin, G.P. Salam and S. Sapeta, *Giant QCD K-factors beyond NLO*, *JHEP* **09** (2010) 084 [[arXiv:1006.2144](#)] [[SPIRES](#)].
- [27] K. Rehermann and B. Tweedie, *Efficient identification of boosted semileptonic top quarks at the LHC*, [arXiv:1007.2221](#) [[SPIRES](#)].
- [28] J. Alwall et al., *MadGraph/MadEvent v4: the new web generation*, *JHEP* **09** (2007) 028 [[arXiv:0706.2334](#)] [[SPIRES](#)].
- [29] S. Hoeche et al., *Matching parton showers and matrix elements*, [hep-ph/0602031](#) [[SPIRES](#)].
- [30] T. Gleisberg et al., *Event generation with SHERPA 1.1*, *JHEP* **02** (2009) 007 [[arXiv:0811.4622](#)] [[SPIRES](#)].
- [31] S. Catani, F. Krauss, R. Kuhn and B.R. Webber, *QCD matrix elements + parton showers*, *JHEP* **11** (2001) 063 [[hep-ph/0109231](#)] [[SPIRES](#)].
- [32] M. Cacciari, G. Salam and G. Soyez, *FastJet*, <http://fastjet.fr/>.
- [33] M. Cacciari and G.P. Salam, *Dispelling the N^3 myth for the k_t jet-finder*, *Phys. Lett. B* **641** (2006) 57 [[hep-ph/0512210](#)] [[SPIRES](#)].
- [34] M. Cacciari, G.P. Salam and G. Soyez, *The anti- k_t jet clustering algorithm*, *JHEP* **04** (2008) 063 [[arXiv:0802.1189](#)] [[SPIRES](#)].
- [35] M.H. Seymour, *Searches for new particles using cone and cluster jet algorithms: a comparative study*, *Z. Phys. C* **62** (1994) 127 [[SPIRES](#)].
- [36] J.M. Butterworth, B.E. Cox and J.R. Forshaw, *WW scattering at the CERN LHC*, *Phys. Rev. D* **65** (2002) 096014 [[hep-ph/0201098](#)] [[SPIRES](#)].
- [37] J.M. Butterworth, J.R. Ellis and A.R. Raklev, *Reconstructing sparticle mass spectra using hadronic decays*, *JHEP* **05** (2007) 033 [[hep-ph/0702150](#)] [[SPIRES](#)].
- [38] Y. Cui, Z. Han and M.D. Schwartz, *W-jet tagging: optimizing the identification of boosted hadronically-decaying W bosons*, [arXiv:1012.2077](#) [[SPIRES](#)].
- [39] T. Han, D. Krohn, L.-T. Wang and W. Zhu, *New physics signals in longitudinal gauge boson scattering at the LHC*, *JHEP* **03** (2010) 082 [[arXiv:0911.3656](#)] [[SPIRES](#)].
- [40] J.M. Butterworth, A.R. Davison, M. Rubin and G.P. Salam, *Jet substructure as a new Higgs search channel at the LHC*, *Phys. Rev. Lett.* **100** (2008) 242001 [[arXiv:0802.2470](#)] [[SPIRES](#)].
- [41] G.D. Kribs, A. Martin, T.S. Roy and M. Spannowsky, *Discovering the Higgs boson in new physics events using jet substructure*, *Phys. Rev. D* **81** (2010) 111501 [[arXiv:0912.4731](#)] [[SPIRES](#)].
- [42] C. Hackstein and M. Spannowsky, *Boosting Higgs discovery — The forgotten channel*, *Phys. Rev. D* **82** (2010) 113012 [[arXiv:1008.2202](#)] [[SPIRES](#)].
- [43] G.D. Kribs, A. Martin, T.S. Roy and M. Spannowsky, *Discovering Higgs bosons of the MSSM using jet substructure*, *Phys. Rev. D* **82** (2010) 095012 [[arXiv:1006.1656](#)] [[SPIRES](#)].

- [44] T. Plehn, G.P. Salam and M. Spannowsky, *Fat jets for a light Higgs*, *Phys. Rev. Lett.* **104** (2010) 111801 [[arXiv:0910.5472](#)] [[SPIRES](#)].
- [45] G.D. Kribs, A. Martin and T.S. Roy, *Higgs discovery through top-partners using jet substructure*, [arXiv:1012.2866](#) [[SPIRES](#)].
- [46] D.E. Kaplan, K. Rehermann, M.D. Schwartz and B. Tweedie, *Top tagging: a method for identifying boosted hadronically decaying top quarks*, *Phys. Rev. Lett.* **101** (2008) 142001 [[arXiv:0806.0848](#)] [[SPIRES](#)].
- [47] J. Thaler and L.-T. Wang, *Strategies to identify boosted tops*, *JHEP* **07** (2008) 092 [[arXiv:0806.0023](#)] [[SPIRES](#)].
- [48] L.G. Almeida et al., *Substructure of high- p_T jets at the LHC*, *Phys. Rev. D* **79** (2009) 074017 [[arXiv:0807.0234](#)] [[SPIRES](#)].
- [49] L.G. Almeida, S.J. Lee, G. Perez, I. Sung and J. Virzi, *Top jets at the LHC*, *Phys. Rev. D* **79** (2009) 074012 [[arXiv:0810.0934](#)] [[SPIRES](#)].
- [50] S.D. Ellis, C.K. Vermilion and J.R. Walsh, *Techniques for improved heavy particle searches with jet substructure*, *Phys. Rev. D* **80** (2009) 051501 [[arXiv:0903.5081](#)] [[SPIRES](#)].
- [51] S.D. Ellis, C.K. Vermilion and J.R. Walsh, *Recombination algorithms and jet substructure: pruning as a tool for heavy particle searches*, *Phys. Rev. D* **81** (2010) 094023 [[arXiv:0912.0033](#)] [[SPIRES](#)].
- [52] L.G. Almeida, S.J. Lee, G. Perez, G. Sterman and I. Sung, *Template overlap method for massive jets*, *Phys. Rev. D* **82** (2010) 054034 [[arXiv:1006.2035](#)] [[SPIRES](#)].
- [53] D. Krohn, J. Shelton and L.-T. Wang, *Measuring the polarization of boosted hadronic tops*, *JHEP* **07** (2010) 041 [[arXiv:0909.3855](#)] [[SPIRES](#)].
- [54] T. Plehn, M. Spannowsky, M. Takeuchi and D. Zerwas, *Stop reconstruction with tagged tops*, *JHEP* **10** (2010) 078 [[arXiv:1006.2833](#)] [[SPIRES](#)].
- [55] J.M. Butterworth, J.R. Ellis, A.R. Raklev and G.P. Salam, *Discovering baryon-number violating neutralino decays at the LHC*, *Phys. Rev. Lett.* **103** (2009) 241803 [[arXiv:0906.0728](#)] [[SPIRES](#)].
- [56] A. Falkowski, D. Krohn, L.-T. Wang, J. Shelton and A. Thalapillil, *Unburied Higgs*, [arXiv:1006.1650](#) [[SPIRES](#)].
- [57] C.-R. Chen, M.M. Nojiri and W. Sreethawong, *Search for the elusive Higgs boson using jet structure at LHC*, *JHEP* **11** (2010) 012 [[arXiv:1006.1151](#)] [[SPIRES](#)].
- [58] A. Katz, M. Son and B. Tweedie, *Jet substructure and the search for neutral spin-one resonances in electroweak boson channels*, *JHEP* **03** (2011) 011 [[arXiv:1010.5253](#)] [[SPIRES](#)].
- [59] C. Englert, C. Hackstein and M. Spannowsky, *Measuring spin and CP from semi-hadronic ZZ decays using jet substructure*, *Phys. Rev. D* **82** (2010) 114024 [[arXiv:1010.0676](#)] [[SPIRES](#)].
- [60] S. Catani, Y.L. Dokshitzer, M.H. Seymour and B.R. Webber, *Longitudinally invariant K_t clustering algorithms for hadron hadron collisions*, *Nucl. Phys. B* **406** (1993) 187 [[SPIRES](#)].
- [61] S.D. Ellis and D.E. Soper, *Successive combination jet algorithm for hadron collisions*, *Phys. Rev. D* **48** (1993) 3160 [[hep-ph/9305266](#)] [[SPIRES](#)].
- [62] J. Gallicchio et al., *Comprehensive multivariate discrimination and the Higgs + W/Z search*, [arXiv:1010.3698](#) [[SPIRES](#)].

- [63] P.E.L. Rakow and B.R. Webber, *Transverse momentum moments of hadron distributions in QCD jets*, *Nucl. Phys. B* **191** (1981) 63 [[SPIRES](#)].
- [64] J. Thaler and K. Van Tilburg, *Identifying boosted objects with N -subjettiness*, *JHEP* **03** (2011) 015 [[arXiv:1011.2268](#)] [[SPIRES](#)].
- [65] J.-H. Kim, *Rest frame subjet algorithm with SISCone jet for fully hadronic decaying Higgs search*, *Phys. Rev. D* **83** (2011) 011502 [[arXiv:1011.1493](#)] [[SPIRES](#)].
- [66] J.M. Campbell, J.W. Huston and W.J. Stirling, *Hard interactions of quarks and gluons: a primer for LHC physics*, *Rept. Prog. Phys.* **70** (2007) 89 [[hep-ph/0611148](#)] [[SPIRES](#)].
- [67] J. Dolen, *Jet substructure in pp collisions at 7 TeV in CMS*, talk given at the Northwest Terascale Workshop, Oregon, U.S.A. (2011).